Proceedings World Geothermal Congress 2020+1
Reykjavik, Iceland, April - October 2021

Magnetotelluric Investigation of the Kasane Geothermal Area in Northwest Botswana

Calistus D. Ramotoroko[1], Anneke P. Thiede[2], Andreas Junge[2] and Elisha Shemang[1]

[1]Department of Earth & Environmental Sciences, Botswana International University of Science & Technology,

[2]Facheinheit Geophysik, Goethe-Universität

Email address: ramotorokoc@biust.ac.bw

Keywords: Magnetotelluric, Kasane, northwest Botswana, Hotspring, Geothermal

ABSTRACT

Kasane is a famous tourist destination in Botswana. Its pleasant climate especially in spring and summer seasons is always worthy for most visitors and residents. Kasane hot spring at the meeting point of four countries – Botswana, Zambia, Namibia and Zimbabwe, with temperature of 43 to 50 ºC is the only known hot spring which exits in Botswana. It lies at about 145 m south of the Chobe River, northwest Botswana. There are no scientific studies on Kasane hot spring and we do not know of the existence of other hot springs in the area. This research is the first detailed research on hot springs in Botswana and an ongoing effort started early 2017 with the goal of developing a conceptual model for the Kasane geothermal hotspring based on the conductivity distribution at depth. Together with additional geological and geochemical studies, the magnetotelluric results are used to infer a comprehensive understanding about the Kasane geothermal hotspring, particularly the reservoir and the heat source.

The data is acquired by both Phoenix and Metronix MT systems at various sample rates for approximately 12 hrs. The acquired MT time-series data are processed using industry standard processing software, FMTools-Frankfurt university software. After data processing, the 2D and 3D inversions are performed using Egbert and Kelbert's (2012) ModEM code and Rod and Mackie's (2001) magnetotelluric inversion program. The 2-D preliminary results are presented in this paper but not yet interpreted because inversion is ongoing. The results will not only provide geothermal reservoir conditions but also insight into potential efficiency drilling and fracturing in the reservoir.

1. INTRODUCTION

The Kasane hot spring at the meeting point of four countries – Botswana, Zambia, Namibia and Zimbabwe, with temperature of 43 to 50 ºC is the only known hot spring which exists in Botswana. It lies at about 145 m south of the Chobe River, northwest Botswana. The region is inadequately studied by geological mapping (Modie, 2000) only at a regional scale as well as by limited hydrogeochemical sampling recently by Mukwati et al. (2018). There are no other scientific studies that have been undertaken at Kasane hot spring. According to the boat helmsmen and fishermen who frequent Chobe river, usually spouts of water, presumably geysers, are observed during dry seasons when Chobe river water level has gone down. The village elders also confirmed there used to be hot springs somewhere in the middle of the river and sometimes in the offshore not far from the current hot spring. We do not know of the exact locations of these previous hot springs in the area. This research is the first detailed geophysical research on hot springs in Botswana and an ongoing effort started early 2017 with the goal of developing a conceptual model for the Kasane geothermal hot spring based on the conductivity distribution at depth. The regional geology in the study area is the orogenic Ghanzi-Chobe belt (Figure 1) which consists of mainly Karoo basalts, and basal volcanics informally termed the Goha Hills Formation overlain by carbonate bearing siliciclastics named the Chinamba Hills Formation (Modie, 2000; Kinabo et al., 2007). The specific local overall geology of the study area consists of basaltic rocks of Karoo lavas made up of mainly silicate minerals such as plagioclase, clinopyroxene and opaque minerals with othopyroxene and amphibole in trace amounts (Mukwati et al., 2018). According to Mukwati et al., (2018) after a chemical analysis of collected waters, Kasane hot spring results from precipitation and fluids of deep origin. Mukwati et al, 2018 also mentioned the high electrical conductivity ranging from 10,000 to 22,320 µS/cm. It is difficult to state the exact basement composition beneath the Kasane study region due to the 300-m-thick sedimentary cover in northern Botswana (Thomas and Shaw, 1990).

2. METHOD AND RESULTS

Magnetotellurics (MT) is a passive geophysical method and is based on principles of electromagnetic (EM) induction. It was proposed as a geophysical method independently by Tikhonov (1950) and Cagniard (1953), and has since been developed into a powerful tool for basic Earth Science and resource exploration. MT makes use of naturally occurring EM fluctuations. Signals with frequencies below ~ 1 Hz are dominantly a result of the interaction between the solar wind and the Earth's magnetosphere and ionosphere (Simpson & Bahr 2005). During times of strong solar activity, the low-frequency source signal is enhanced, therefore increasing signal-to-noise ratio. MT also makes use of frequencies above ~ 1 Hz. These have their origin in global lightning discharges, especially from the equatorial regions. The EM fields created this way propagate around the world within the waveguide bounded by the ionosphere and the surface of the Earth (Simpson & Bahr 2005). The transition zone between these two source fields at ~ 0.5 – 5 Hz (Egbert & Livelybrooks 1996) is commonly referred to as the MT dead band.

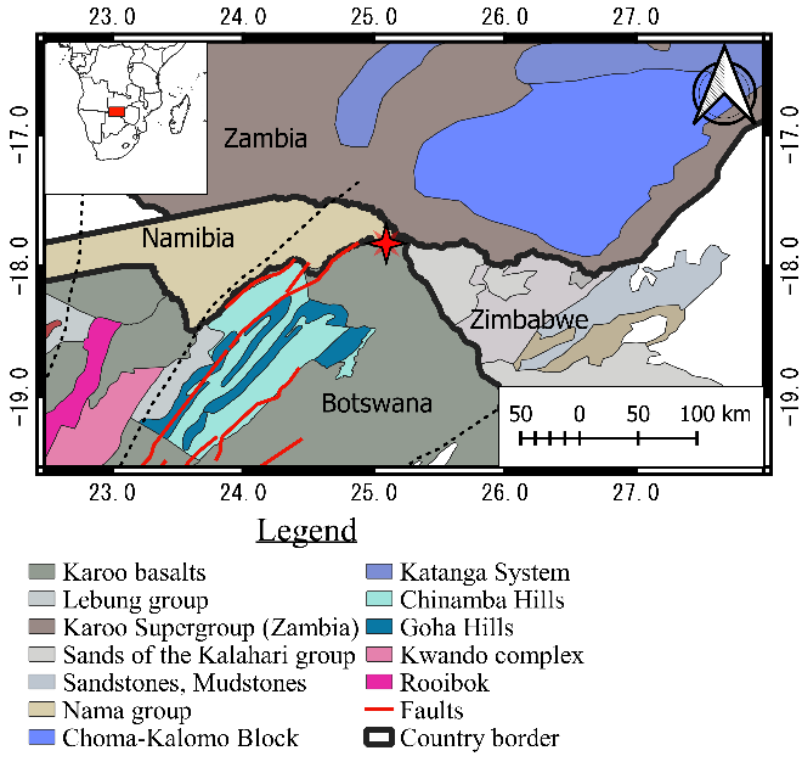

Figure 1. Geological map of the region surrounding Kasane hot spring (red star).

Variation of electrical resistivity below subsurface can be calculated based on the formulations introduced by Cagniard (1953). The impedance Z_{xy} is defined as the ratio of the electric field in the x-direction, E_x and magnetic field in the y-direction, B_y, as:

$$Z_{ij} = \frac{E_i}{B_j} \qquad (1)$$

The subscripts *i* and *j* in the equations above indicate direction of electric and magnetic fields measurements in x and y directions, respectively.

The components of the electric and magnetic fields can be used to calculate the impedance tensor, as:

$$\begin{bmatrix} E_x \\ E_y \end{bmatrix} = \begin{bmatrix} Z_{xx} & Z_{xy} \\ Z_{yx} & Z_{yy} \end{bmatrix} \begin{bmatrix} B_x \\ B_y \end{bmatrix} \qquad (2)$$

Formally, the apparent resistivity (ρ_a) and phase (φ) can be calculated based on the impedance elements (Z) for an equivalent half space, i.e.

$$\rho_{a,ij} = \frac{1}{\omega \mu_0} |Z_{ij}|^2 \qquad (3)$$

and

$$\varphi_{ij} = \tan^{-1}\left(\frac{Im(Z_{ij})}{Re(Z_{ij})}\right) \qquad (4)$$

where Z = magnetotelluric impedance in m/s, $\mu_0 = 1.2566 \times 10^{-6}$ [H/m] the magnetic permeability in free space, φ is the phase in rad and ω is frequency in Hz.

The vertical magnetic field can be related to the horizontal magnetic fields through the so called tipper, **T**. which is a complex vector and defined as following:

$$H_z = (T_x(w) \;\; T_y(w)) \begin{pmatrix} H_x \\ H_y \end{pmatrix} \qquad (5)$$

Induction arrows can be used to graphically represent this vector in order to identify lateral resistivity variations that give rise to the vertical magnetic field. The most commonly adopted convention for the orientation for these arrows is the Parkinson convention, where the real arrows are reversed so that they point towards high concentrations of current and therefore areas of high conductivity

(Parkinson 1959). The alternative convention is the Wiese convention (Wiese 1962), where the arrows are unreversed so that the real arrows point away from current concentrations in conducting bodies. The imaginary arrows go through a reversal pointing away from the conducting body at high frequencies, going through zero at the period that maximises the real arrow, then pointing towards the anomaly at longer at longer periods.

A geothermal system is made up of a heat source, a reservoir and fluids that absorb and transfer the heat. A magmatic intrusion at shallow depths, usually 4 – 5 km (Patro 2017) is believed to be the main heat source. Geothermal systems, in general, are associated with structures such as faults, fractures and shear zones which act as conduits for the circulation of geothermal fluids in the rock matrix of the system. Very often these fluids, because of dissolved salts, act as electrically conducting electrolytes, thus imparting a conductive nature to the structural features. As temperature affects the mineral composition of rocks, it may influence the conductivity of a geothermal system. At temperatures between 70 to 200ºC the highly conductive clay smectite is the predominant alteration mineral that is produced, and it is therefore the most likely to be found outside the reservoir itself and away from the highest temperatures (Cherkose & Mizunaga 2017). The electromagnetic and electrical methods can provide a model of the subsurface resistivity variation. As we like to investigate the geothermal situation to greater depths, MT is the appropriate method applied to provide a model of the subsurface resistivity. It has been successfully used in geothermal investigations (Wright et al., 1985; Volpi et al., 2003; Pellerin et al., 1996; Heise et al. 2008; Newman et al., 2008; Liddell, 2014; Woitischek et al. 2017).

The field work to collect the magnetotelluric dataset for this research project was carried out in November 2017 and July 2018. A total of 24 measurements were collected (Figure 2). The site spacing was on average 1 km with the array spanning 10 x 3 km.

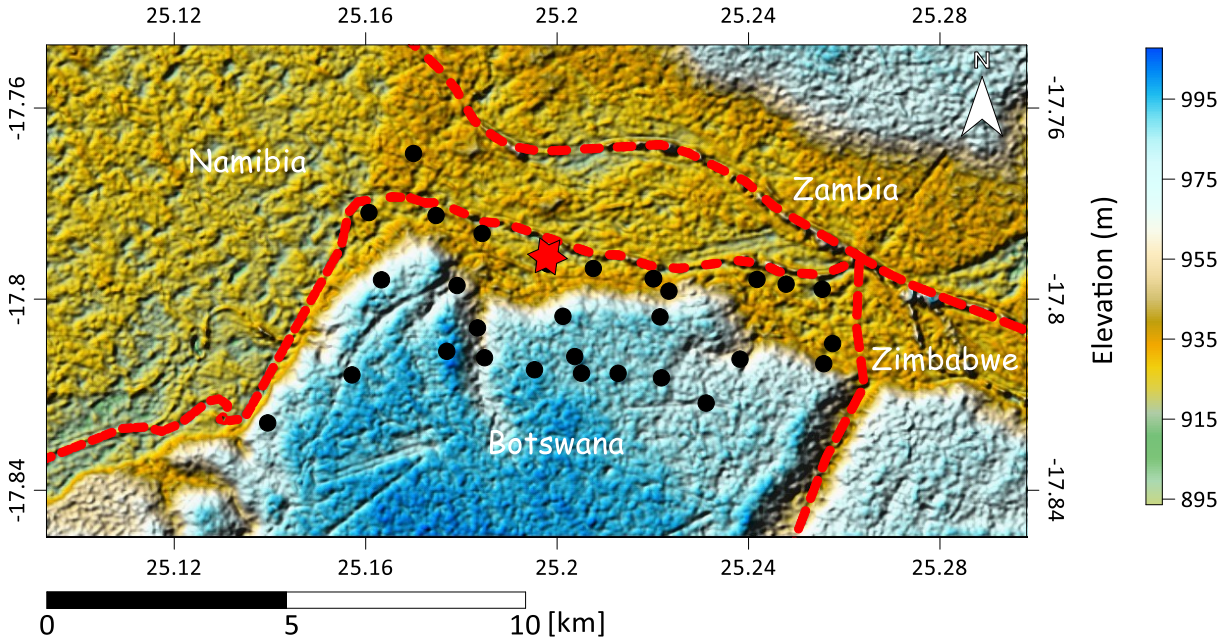

Figure 2. The topographic map showing the locations of the magnetotelluric stations (black filled circles). The dashed red lines mark the international borders. The hot spring location is indicated by red star.

The data are acquired using Phoenix Geophysics' MTU-5A, and Metronix's ADU07 and ADU07e MT systems at various sample rates. The Metronix ADU systems were used as local sites measured at sampling frequencies of 2048 Hz and 16384 Hz whilst the MTU-5A was placed at 10 km distance as remote site measured continuously with 150 Hz and discontinuously with 2400 Hz and 24000 Hz. A notch filter at 50 Hz was switched on for the MTU-5A because of power line noise. The magnetic field temporal variations were measured using MTC-150L coils from Phoenix Geophysics with an acquisition range of 0.0001 Hz to 10 kHz whilst MFS07e coils with an acquisition range of 0.001 Hz up to 50 kHz were used in Metronix systems. The electric field variations were measured using non-polarized potassium chloride (KCl)) electrodes for Metronix instruments and sodium chloride (NaCI) electrodes for Phoenix instrument. The dipole lengths were varied between 30 to 100 m for all the sites, depending on the accessibility. The three instruments were recording synchronously for 12 hrs per day. For the two Metronix instruments (ADU07, ADU07e), one measured electric field (Ex and Ey) components only whilst the other instrument measured two electric and two horizontal magnetic components (Ex, Ey, Bx By). All the five MTU-5A components (Ex, Ey, Bx, By, Bz) were measured. In all cases, where data from a remote site are available, the remote magnetic fields will be used in the impedance estimation of the local site.

Since magnetotellurics (MT) is a passive geophysical method that relies on naturally occurring electromagnetic waves, it is often highly sensitive to cultural electric, and to a somewhat lesser extent magnetic, noise. Especially in a town like Kasane that is within wildlife territory, cultural noise due to electric fences is one of the major issues for magnetotelluric measurements. In the Kasane region, cultural noise is not only caused by electric fences but also powerlines as well as industrial power generators and machinery. A segment of the first 3 seconds from the three instruments is shown in Figure 3 below.

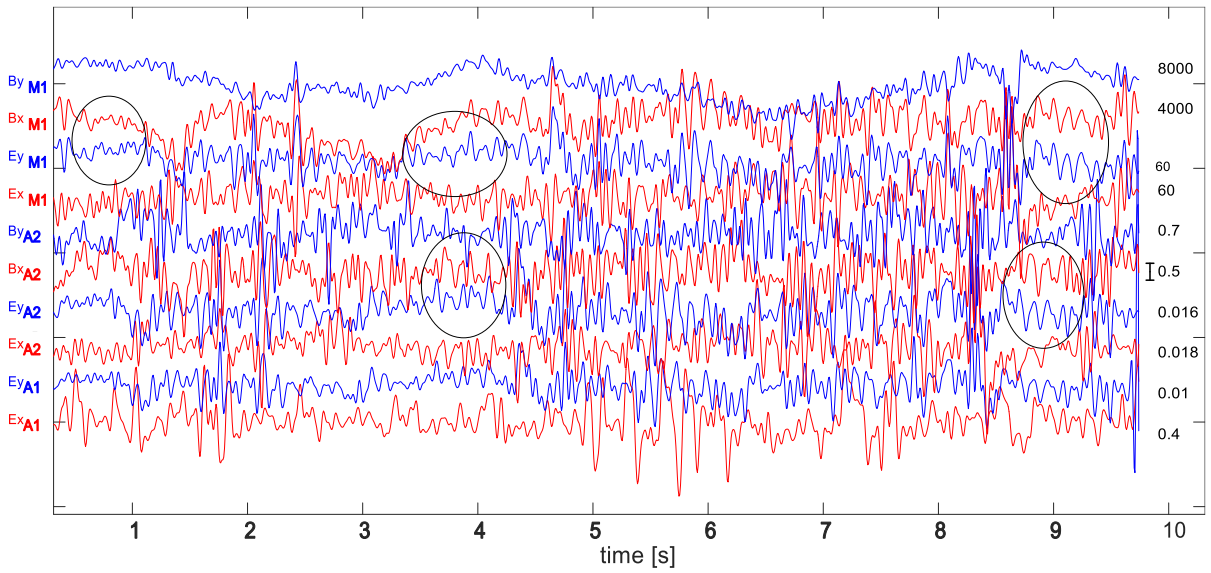

Figure 3. Time series for 5 channel MTU-5A, ADU-07 two channels and ADU-07e four channel of magnetotelluric data from site9_MTU_5A, site9_ADU_2Ch and site9_ADU_4Ch respectively. Ex and Ey are the two orthogonal horizontal components of the electric field. Bx, and By are the components of the horizontal magnetic field. Note the correlation between Bx and Ey, and between By and Ex (indicated by black cirlces). The time series presented is that of the MTU-5A (M1) at sampling rate 150 Hz and at 2048 Hz for Metronix instruments (A1 and A2) measured synchronously. Time is measured from 17:05:56 UTC +2, on July 30, 2018. All units are normalized.

The MATLAB (the MathWorks, Inc.) scripts, within Frankfurt University software package, FMTools have been used for the data processing in the current study. The program FMTools builds on an eigenvalue decomposition developed by Egbert (1997). The program is a standard robust processing software that was used to convert time series from time domain to frequency domain and calculate impedance estimates.

At the moment, only apparent resistivity and phase curves for Z_{xy} and Z_{yx} and preliminary 2D model are discussed in this paper.

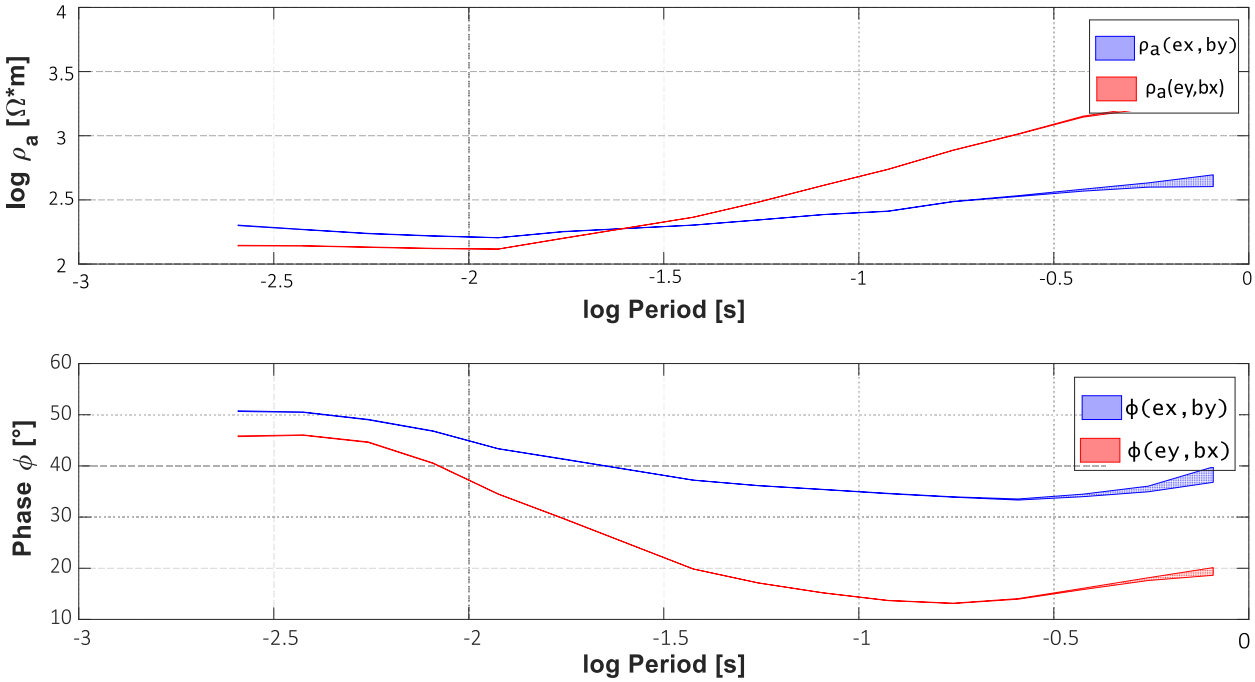

Figure 4. Apparent resistivity and phase curves – from site9 MTU-5A instrument are plotted against period, which acts as a proxy for depth. The symbols ρ_a (e_x, b_y) and ρ_a (e_y, b_x) represent apparent resistivities calculated from Z_{xy} and Z_{yx} and their corresponding phase curves $\varphi(e_x, b_y)$ and $\varphi(e_y, b_x)$ respectively. The shaded area reflects the standard deviation. Note the log scales for both apparent resistivity and period.

Owing to the Kasane and Kazungula towns close the measurement area, electromagnetic noise was experienced at some sites. To reduce noise, we chose a field schedule to apply remote reference with the Phoenix system as remote, so multiple site processing is yet to be executed. At the moment, only apparent resistivity and phase curves for Z_{xy} and Z_{yx} obtained from single site processing are discussed in this paper.

Most MT resistivity curves observed in the study area have a similar trend as that of site9 shown in Figure 4. The apparent resistivity at site9 is relatively low ~300 Ω.m at the shortest periods (<0.01 s), which represents a depth range down to approx. 0.5 km. The resistivity then increases to very high values ~5000 Ω.m from 0.01 s to the longest periods, indicating a strong resistor located deep in the subsurface. In theory, the phase angle is at 45° for a homogeneous half space and it decreases if the resistivity increases with depth. This is consistent with the observation (Figure 4). The split in the phase indicates lateral changes of the conductivity distribution causing the directional dependency of the impedances.

The phase tensor method is used for tensor decomposition for dimensionality analysis. See detailed explanation of the underlying theory described by Caldwell et al. (2004). The phase tensor results are displayed in map view below (Figure 5a and 5b).

At high frequencies (Figure 5a) most of the phase tensors plot as circles or very close to circular, indicating that there is no defined strike at the shallow depths sampled by these EM signals.

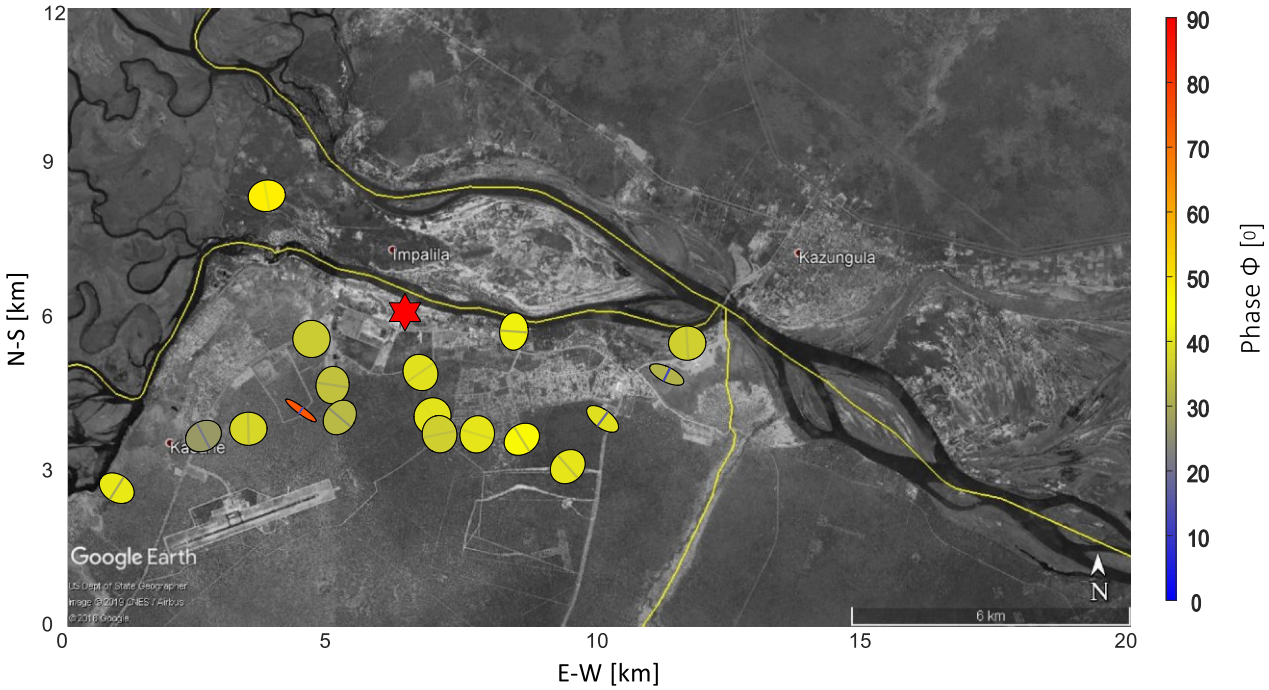

Figure 5a. Map of phase tensor ellipses at the study area at high frequencies (144 Hz). Ellipse fill color is the phase for the long ellipse principal axis, the color of the bar within the ellipse reflects the short principal axis. The red star marks the hot spring location.

At lower frequencies, for example at 13.7 Hz (Figure 5b) the phase tensors appear more elliptical, with a preferred strike direction of N45°E.

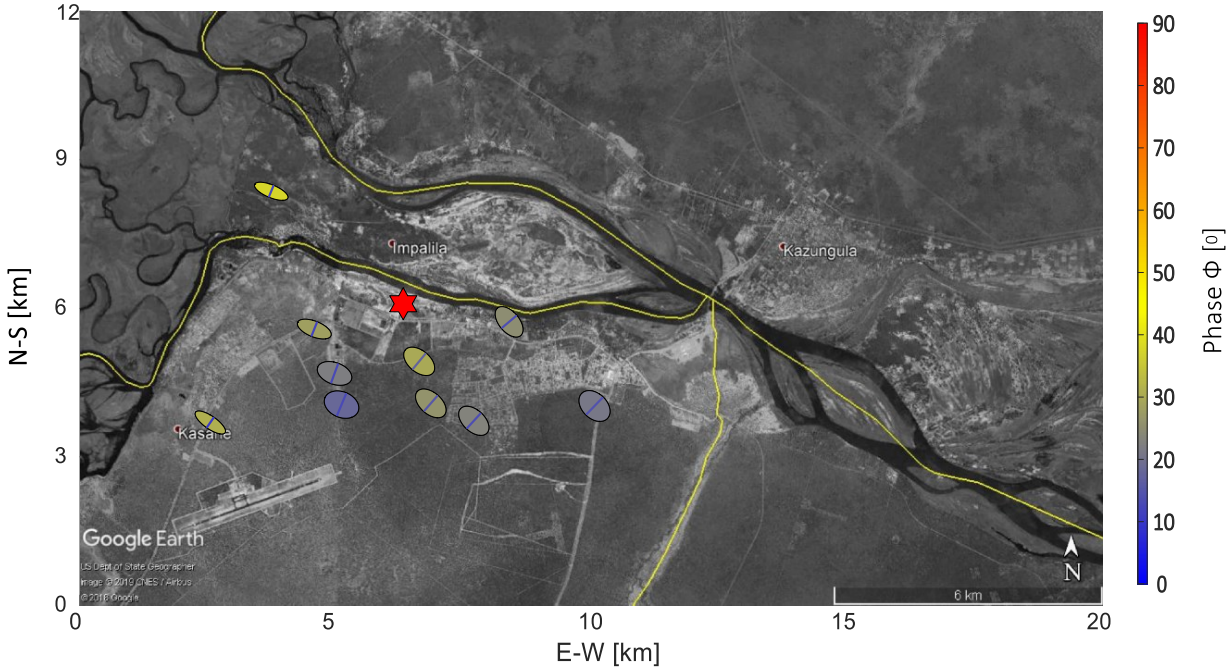

Figure 5b. Map of phase tensor ellipses at the study area at low frequencies (13.7 Hz). Further description cf Figure. 5a. The red star marks the hot spring location.

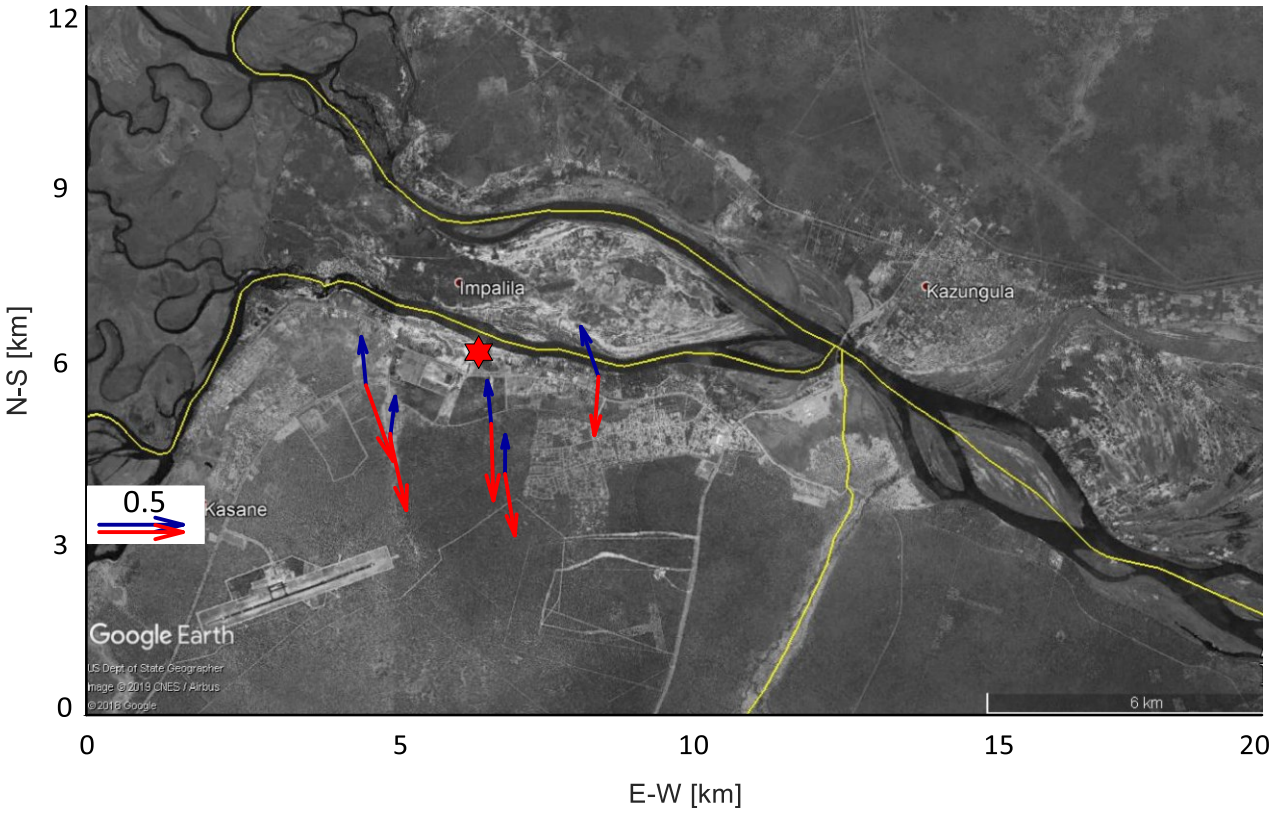

Figure 6. Induction arrows at 1.3 Hz, plotted using the convention by Wiese (1962) at different periods superimposed on Google earth map of the region. The red star marks the hot spring location.

Figure 6 above shows the induction arrows at lower frequency (1.3 Hz) for some of the sites in the survey area. The induction arrows points to the south, away from the most likely conductive geothermally altered zone in the north i.e. away from hot spring.

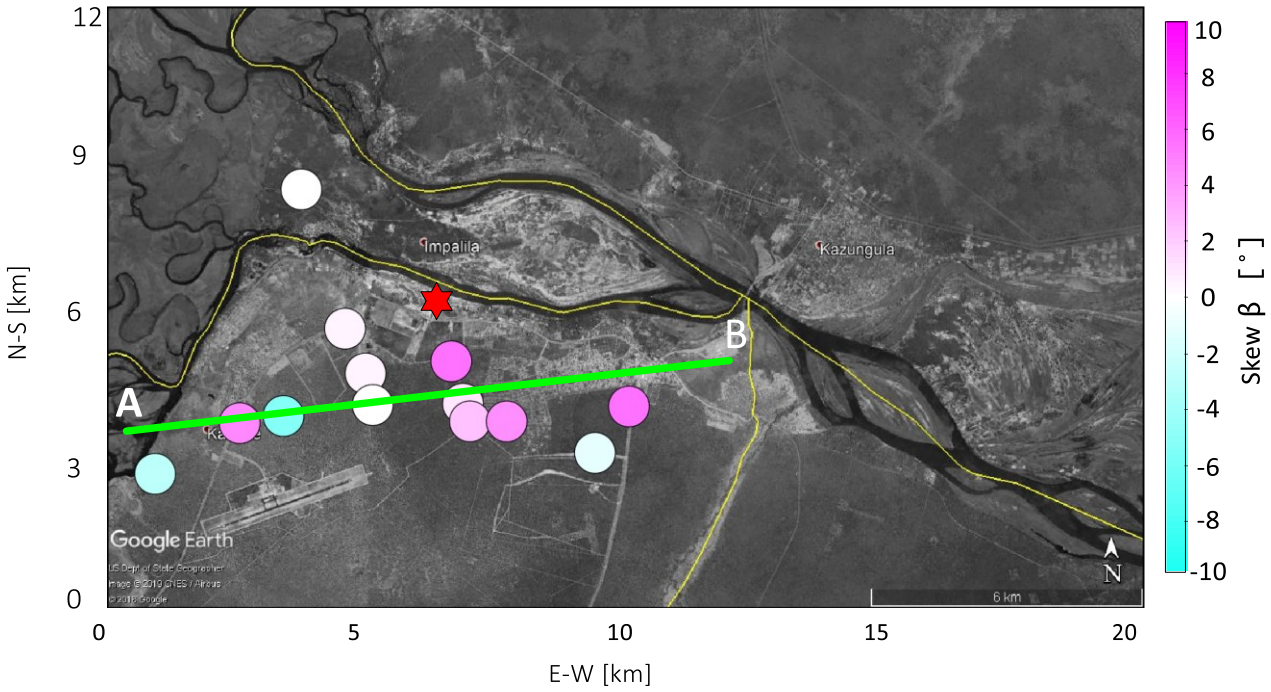

Figure 7. Map of skew (β) values at 1519 Hz frequency, calculated using algorithm described by Caldwell et al., 2005. Green line A-B represents profile used for 2D inversion. The red star marks the hot spring location.

Skew values calculated using algorithm explained in Caldwell et al. (2004) are generally between 1 and 4° at a few sites notably in the central part of the study area, close to the hot spring. Skew values within this range indicate a 2-D conductivity distribution within the subsurface near that location. We shall investigate this assumption by 3D modelling studies.

The magnetotelluric data acquired are inverted using WinGlink 2D inversion program (Rodi and Mackie, 2001) and 3-D inversion is carried out using a parallel version of ModEM (Egbert and Kelbert, 2012). All but three MT stations are used in the 2-D and 3-D inversion modelling.

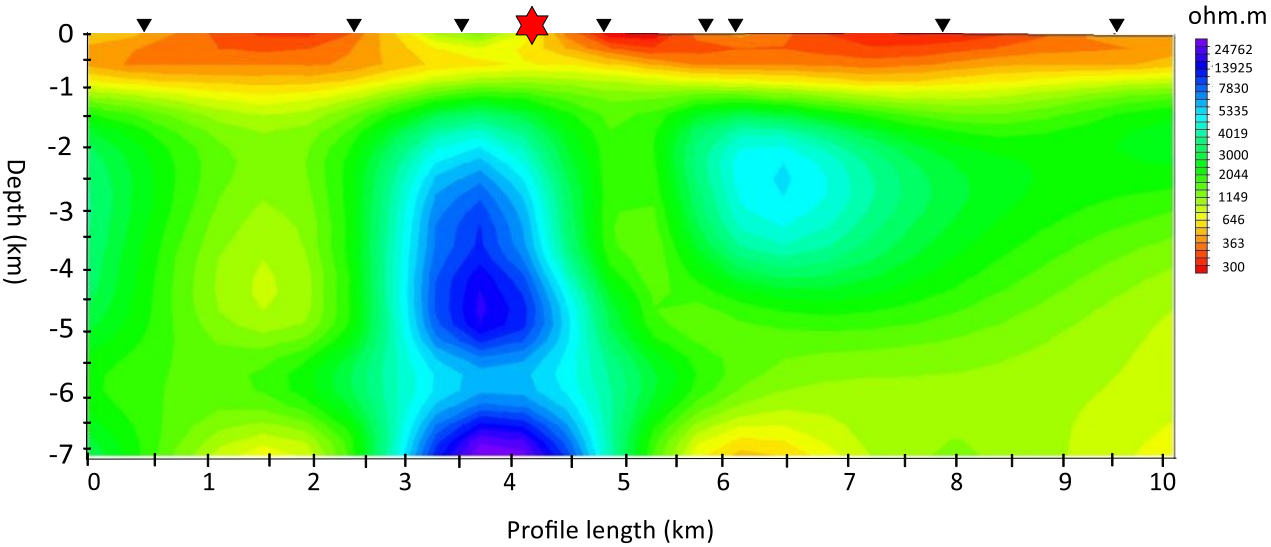

Figure 8: 2-D inversion result for profile along Chobe river (see Figure 7). The red star represent hot spring location.

The results of 2-D inversion reveal a thick prominent conductive layer above a highly distinct resistive 'up-doming' structure at depth, located in the central part of the survey area (see Figure 7) where the hot spring is found. The 3D inversions are currently running. Concrete 2D and 3D results, and interpretation will be ready at the time of the conference.

3. CONCLUSIONS

The analysis of preliminary resistivity curves shows a shallow conductive layer which may be interpreted as conductive smectite. The conductive top layer is underlain by a higher resistive structure as expected. Various studies of the resistivity distribution in high temperature geothermal systems around the world have shown similar models (cf Hogg et al., 2018, and citations therein).

ACKNOWLEDGMENTS

We would like to thank the Office of Research, Development & Innovation (BIUST) and Institute of Geosciences, Frankfurt University for financing the research. We thank Metronix for providing the ADU coils.

REFERENCES

Cagniard, L.: Basic theory of the magneto-telluric method of geophysical prospecting, *Geophysics*, **18**, (1953), 605-635.

Caldwell, T.G., Bibby, H.M., and Brown, C.: The magnetotelluric phase tensor, *Geophysical Journal International*, **158**, (2004), 457–469.

Cherkose, B.A., and Mizunaga, H.: Resistivity imaging of Aluto-Langano geothermal field using 3-D magnetotelluric inversion, *Journal of African Earth Sciences*, **139**, (2018), 307-318. https://doi.org/10.1016/j.jafrearsci.2017.12.017

Egbert, G.D. and Livelybrooks, D.W.:Single station magnetotelluric impedance estimation: Coherence weighting and the regression M-estimate. *Geophysics*, **61**, (1996), 964-970.

Egbert, G. D.: Robust multiple-station magnetotelluric data processing. *Geophysical Journal International*, **130**, (1997) 475–496.

Egbert, G., and Kelbert, A.: Computational recipes of electromagnetic inverse problems, *Geophysical Journal International*, **189**, (2012), 251-267.

Heise, W., Caldwell, T. G., and Bibby, S. C.: Three-dimensional modelling of magnetotelluric data from the Rotokawa geothermal field, Taupo Volcanic Zone, New Zealand, *Geophysical Journal International*. **173**, (2008), 740-750.

Hogg, C., Kiyan, D., Rath, V., Byrdina, S., Vandemeulebrouck, J., Revil, A., Viveiros, F., Carmo, R., Siva., and Ferreira, T.:3D interpretation of short-period magnetotelluric data at Furnas volcano, Azores Islands, *Geophysics Journal International*, **213** (2018), 371-386.

Kinabo B.D., Atekwana E.A., Hogan J.P., Modisi M.P., Wheaton D.D., and Kampunzu A.B.: Early structural development of the Okavango rift zone, NW Botswana. *Journal of African Earth Sciences*, **48**, (2007), 125–136.

Liddell, M.V. 2014 Magnetotelluric Imaging of Electrically Anisotropic Crust Near Fort McMurray, Alberta, *MSc Thesis*, Dept of Physics, University of Alberta.

MATLAB and Statistics Toolbox Release 2019a, *The MathWorks*, Inc., Natick, Massachusetts, United States.

Modie, B. N., Geology and mineralisation in the Meso-to Neopro-terozoic Ghanzi-Chobe belt of northwest Botswana: *Journal of African Earth Sciences*, **30**, (2000) 467–474, doi:10.1016/S0899-5362(00)00032-4

Mukwati B. T., Nata T. Tafesse N. T.*, Bagai, Z. B., and Laletsang K.: Hydrogeochemistry of the Kasane Hot Spring, Botswana. *Universal Journal of Geoscience,* **6**, (2018), 131-146, doi: 10.13189/ujg.2018.060501

Newman, G.A., Gasperikova, E., Hoversten, G.M., Wannamaker, P.E.: Three dimensional magnetotelluric characterization of the Coso geothermal field. *Geothermics,* **37**, (2008), 369–399.

Parkinson, W.: Direction of rapid geomagnetic variations, *Geophysical Journal of the Royal Astronomical Society*, **2**, (1959), 1-14.)

Pellerin, L., Johnston, J. M., & Hohmann, G. W.: A numerical evaluation of electromagnetic methods in geothermal exploration. *Geophysics*, **61**, (1996), 121–130.

Rodi, W. and Mackie, R. L.: Nonlinear conjugate gradients algorithm for 2-D magnetotelluric inversion. *Geophysics*, **66**, (2001), 174-187.

Thomas, D. S. G., and Shaw, P. A.: The deposition and development of the Kalahari Group sediments, Central Southern Africa: *Journal of African Earth Sciences*, **10**, (1990), 187–197, doi: 10.1016/0899-5362(90) 90054-I.

Tikhonov, A.N.: Determination of the electrical characteristics of the deep strata of the Earth's crust, Dok. Akad. Nauk., *USSR*, **73**, (1950), 295-297.

Simpson, F. & Bahr, K.: Practical magnetotellurics, Cambridge University Press, (2005).

Volpi, G., Manzella, A., Fiordelisi, A.: Investigation of geothermal structures by magnetotellurics (MT): an example from the Mt. Amiata area, Italy. *Geothermics* **32**, (2003), 131–145.

Wiese, H., Geomagnetische Tiefentellurik, 2, Die Streichrichtung der Untergrundstrukturen des elektrischen Widerstandes, erschlossen aus geomagnetischen Variationen, *Geofis. Pura Appl*., **52**, (1962), 83.

Woitischek, J. Dietzel, M., Inguaggiato, C., Böttcher, M., Leis, A., Cruz, J. V. and Gehre, M.: Characterisation and origin of hydrothermal waters at Sao Miguel (Azores) inferred by chemical and isotopic composition, *Journal of Volcanology and Geothermal Research*, **46**, (2017), DOI: 10.1016/j.jvolgeores.2017.03.020

Wright, P.M.,Ward, S.H., Ross, H.P., West, R.C.: State-of-the-art geophysical exploration for geothermal resources *Geophysics*, **50**, (1985), 2666–2696.

Zhang, L. Hao, T., Xiao, Q., Wang, J., Zhou, L., Qi, M., Cui, X., Cai, N.: Magnetotelluric investigation of the geothermal anomaly in Hailin, Mudanjiang, northeastern China. *Journal of Applied Geophysics*, **118**, (2015), 47–65 http://dx.doi.org/10.1016/j.jappgeo.2015.04.006